

Department of Pharmacology

# Qualifying Examination (Part I)

July 19-23, 2010

Please remember that this is a closed-book examination. You must be prepared to answer 4 of the 7 questions. Although not necessary, you may prepare written answers, overhead figures, or any type of materials that you think might be useful in the presentation of your answers. You may bring such preparation materials with you to the examination. The oral examination itself will not extend beyond two hours.

Full therapeutic benefit of antidepressant treatment is only achieved after several weeks of treatment. Chronic treatment with antidepressant drugs stimulates neurogenesis in the adult hippocampus. Antidepressants increase neural progenitor proliferation and induce morphological maturation of newborn neurons. Activation of neurogenesis requires 2–3 weeks of sustained antidepressant administration and has been demonstrated to play an important role in the behavioral effects of antidepressants.

Experiments were conducted to investigate the role of adrenergic receptors in the effects of antidepressants. Some of the results are presented in Figures 1 and 2 below.

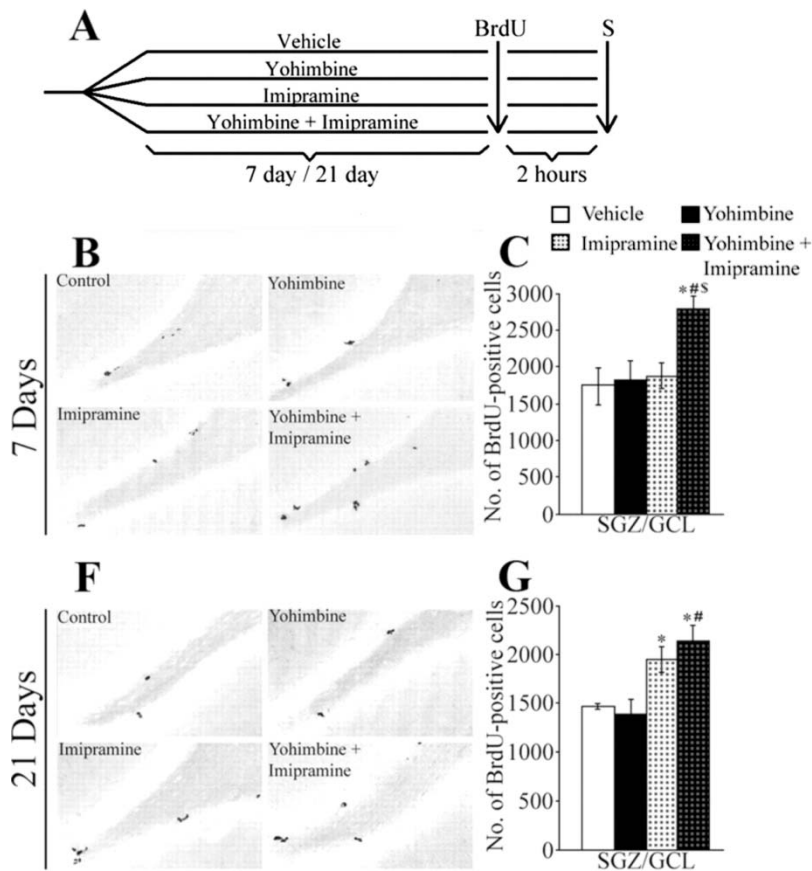


**Figure 1.** The effect of the  $\alpha_2$ -adrenoceptor blockade on the imipramine-induced progenitor proliferation in the adult rat hippocampus. Rats received combined treatment with the  $\alpha_2$ -adrenoceptor antagonist, yohimbine, and the tricyclic antidepressant imipramine for 7 or 21 days. **A**, Shown is a schematic representation of the experimental design (S - time point for sacrificing the animals). Influence of 7 or 21 d combined yohimbine and imipramine treatments on adult hippocampal neurogenesis was assessed using the mitotic marker BrdU (bromodeoxyuridine). **B**, **F**, Representative photomicrographs of BrdU-positive cells from control-, yohimbine-, imipramine-, and yohimbine + imipramine-treated groups from the 7 d (**B**) and 21 d (**F**) experiments. **C**, Quantitative analysis of the number of BrdU-positive cells in the SGZ/GCL (subgranular zone/granular cell layer) of the dentate gyrus of animals that received short duration 7 d combined treatments with yohimbine and imipramine. **G**, Quantitative analysis of the number of BrdU-positive cells in the SGZ/GCL (subgranular zone/granular cell layer) of the dentate gyrus of animals that received long duration 21 d combined treatments with yohimbine and imipramine. \* $p < 0.05$  compared with vehicle, # $p < 0.05$  compared with yohimbine, \$ $p < 0.05$  compared with imipramine (ANOVA and Bonferroni *post hoc* test).

**A**

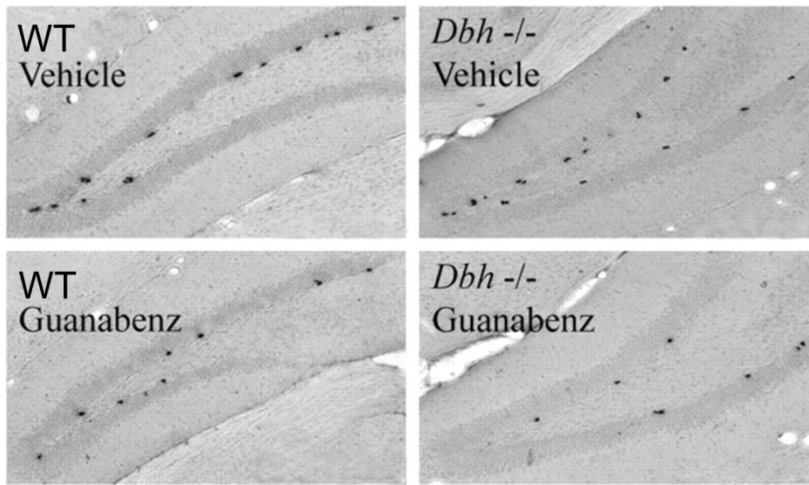
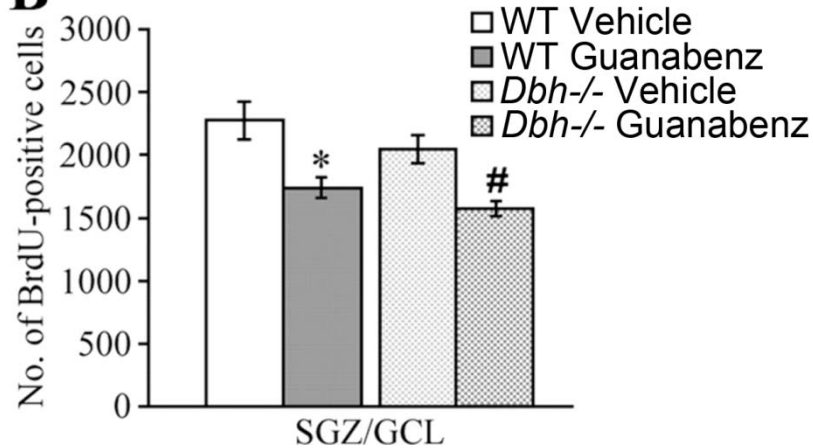


**Figure 2.** The effect of the  $\alpha_2$ -adrenoceptor stimulation on neurogenesis in the adult hippocampus of wild type mice and mice lacking dopamine- $\beta$ -hydroxylase ( $Dbh^{-/-}$ ). WT and  $Dbh^{-/-}$  mice received treatment with  $\alpha_2$ -adrenoceptor agonist guanabenz or vehicle once daily for 7 days. **A**, Representative photomicrographs of BrdU-positive cells from vehicle- and guanabenz-treated WT and  $Dbh^{-/-}$  animals. **B**, Quantitative analysis of the number of BrdU-positive cells in the SGZ/GCL of WT and  $Dbh^{-/-}$  mice following guanabenz treatment. \* $p < 0.05$  compared with WT vehicle; # $p < 0.05$  compared with  $Dbh^{-/-}$  vehicle (ANOVA and Bonferroni *post hoc* test).

**B**



1. What neurotransmitter system(s) and protein(s) are targeted by imipramine? Based on Figs. 1&2, what is the contribution of  $\alpha_2$ -adrenergic receptors to the neurogenesis-inducing effect of imipramine?
2. What neurotransmitter system(s) is affected and how in mice lacking dopamine- $\beta$ -hydroxylase? What is the effect of the  $\alpha_2$ -adrenoreceptor stimulation on hippocampal neurogenesis in  $Dbh^{-/-}$  mice as compared to wild type (Fig. 2)? What do these results tell about the role of  $\alpha_2$ -adrenoreceptors in the hippocampal neurogenesis? Propose two additional experiments to further clarify the role of  $\alpha_2$ -adrenoreceptors in the hippocampal neurogenesis

Pregnant women have reduced exposure (AUC) to the anti-HIV protease inhibitor Nelfinavir (NFV). In attempting to model this in mice, NFV was administered orally and intravenously to timed pregnant (18-19-day) mice and non-pregnant mice, and the following results were obtained:

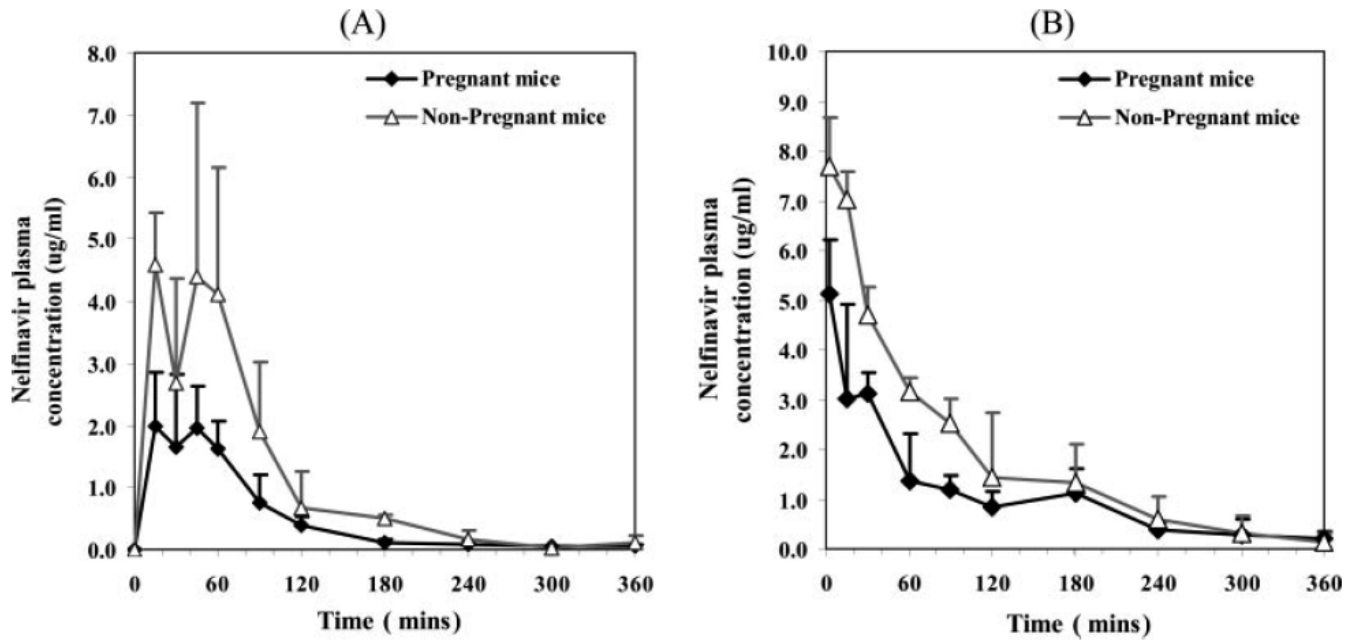


**Fig. 1.** NFV plasma concentration-time profiles (mean  $\pm$  S.D.,  $n = 6$  per time point) after (A) oral (2.5 mg) or (B) i.v. (0.625 mg) administration of NFV to timed pregnant (gestational age: 18–19 days) and nonpregnant FVB mice. NFV plasma concentration- time profiles in pregnant mice are significantly lower ( $p < 0.05$ ) than those in nonpregnant mice after oral but not after i.v. administration of the drug.

**TABLE 1**  
Pharmacokinetic parameters (means  $\pm$  S.D.) of NFV after oral administration of NFV (2.5 mg) to pregnant (gestational age: 18–19 days) and nonpregnant FVB mice

| Parameters                            | Pregnant Mice ( $n = 6$ ) | Nonpregnant Mice ( $n = 6$ ) | $p$ Value <sup>d</sup> |
|---------------------------------------|---------------------------|------------------------------|------------------------|
| AUC <sub>0-∞</sub> (μg/ml/min)        | 176.5 $\pm$ 43.2          | 396.8 $\pm$ 31.7             | 0.002                  |
| CL/F (ml/min) <sup>b</sup>            | 14.8 $\pm$ 4.0            | 6.3 $\pm$ 0.5                | 0.022                  |
| CL/F (ml/min/g)                       | 0.6 $\pm$ 0.2             | 0.3 $\pm$ 0.02               | 0.020                  |
| CL/F unbound (ml/min) <sup>c</sup>    | 1107.1 $\pm$ 297.2        | 209.5 $\pm$ 17.4             | 0.006                  |
| CL/F unbound (ml/min/g)               | 44.2 $\pm$ 11.5           | 8.4 $\pm$ 0.7                | 0.006                  |
| C <sub>max</sub> (μg/ml) <sup>d</sup> | 2.6 $\pm$ 0.3             | 6.2 $\pm$ 1.4                | 0.011                  |
| $t_{1/2}$ (min) <sup>e</sup>          | 77.9 $\pm$ 4.5            | 70.4 $\pm$ 43.4              | 0.782                  |
| $F$ (%) <sup>f</sup>                  | 10.8 $\pm$ 2.6            | 15.7 $\pm$ 1.3               | 0.043                  |
| fp (% unbound) <sup>g</sup>           | 1.3 $\pm$ 0.1             | 3.0 $\pm$ 1.4                | 0.049                  |

<sup>a</sup> Parameters were compared using the two-sample  $t$  test (equal variance, statistical significance  $p < 0.05$ ).

<sup>b</sup> Total oral plasma clearance.

<sup>c</sup> Unbound oral plasma clearance.

<sup>d</sup> Maximum plasma concentration.

<sup>e</sup> Terminal plasma half-life.

<sup>f</sup> Bioavailability.

<sup>g</sup> Percent unbound in plasma.

Qualifying Exam – July 2010  
Question 2

TABLE 2

Pharmacokinetic parameters (means  $\pm$  S.D.) of NFV after i.v. administration of NFV (0.625 mg) to pregnant (gestational age: 18–19 days) and nonpregnant FVB mice

| Parameters                                  | Pregnant Mice ( $n = 6$ ) | Nonpregnant Mice ( $n = 6$ ) | $p$ Value <sup>a</sup> |
|---|---------------------------|------------------------------|------------------------|
| AUC <sub>0-∞</sub> (μg/ml/min)              | 411.2 $\pm$ 68.5          | 645.8 $\pm$ 106.3            | 0.023                  |
| CL(ml/min) <sup>b</sup>                     | 1.6 $\pm$ 0.3             | 1.0 $\pm$ 0.2                | 0.047                  |
| CL (ml/min/g)                               | 0.1 $\pm$ 0.01            | 0.04 $\pm$ 0.01              | 0.037                  |
| CL <sub>unbound</sub> (ml/min) <sup>c</sup> | 60.7 $\pm$ 10.5           | 40.4 $\pm$ 8.0               | 0.052                  |
| CL <sub>unbound</sub> (ml/min/g)            | 2.5 $\pm$ 0.3             | 1.7 $\pm$ 0.3                | 0.052                  |
| V <sub>ss</sub> (ml) <sup>d</sup>           | 208.3 $\pm$ 57.1          | 100.6 $\pm$ 35.6             | 0.046                  |
| V <sub>ss</sub> (ml/g)                      | 8.6 $\pm$ 2.2             | 4.2 $\pm$ 1.6                | 0.045                  |
| $t_{1/2}$ (min) <sup>e</sup>                | 94.4 $\pm$ 27.9           | 71.2 $\pm$ 32.2              | 0.465                  |
| fp (% unbound) <sup>f</sup>                 | 2.6 $\pm$ 0.7             | 2.5 $\pm$ 0.3                | 0.801                  |

<sup>a</sup> Parameters were compared using the two-sample  $t$  test (equal variance, statistical significance  $p < 0.05$ ).

<sup>b</sup> Clearance.

<sup>c</sup> Unbound clearance.

<sup>d</sup> Volume of distribution at steady state.

<sup>e</sup> Terminal plasma half-life.

<sup>f</sup> Percent unbound in plasma.

- 1. Briefly review and evaluate these data.**
- 2. Propose additional experiments to elucidate the mechanisms underlying altered disposition of NFV in pregnant compared to non-pregnant mice.**

*Familial glucocorticoid deficiency (FGD), or hereditary unresponsiveness to adrenocorticotropin results from resistance to the action of ACTH on the adrenal cortex, which stimulates glucocorticoid production. Affected individuals are deficient in cortisol and, if untreated, are likely to succumb to hypoglycemia or overwhelming infection in infancy. Mutations of the ACTH receptor (melanocortin 2 receptor, MC2R), whose stimulation increases intracellular cAMP, account for 25% of cases of FGD. FGD without mutations of MC2R is called FGD type 2. You identify, in a consanguineous family, a mutation in a gene (MC2RAP) encoding a single-transmembrane domain protein, which cause FGD type 2.*

- 1- Using a simple diagram, illustrate how the hypothalamus regulates glucocorticoid production by the adrenal gland.**
- 2- Based on this diagram,**
  - a. What should be the levels of ACTH and CRH in FGD type 2 patients?**
  - b. How would you measure this?**
  - c. Explain the principle of the assay.**
- 3- These patients show hyperpigmentation of the skin. How would you explain this?**
- 4- What are the main tissues and physiologic functions that glucocorticoids regulate?**
- 5- In the past you tried to express MC2R in various cell lines but it proved to be very difficult to obtain MC2R expression and signaling. You now realized that only those cell lines expressing endogenous MC2RAP were able to express a functional MC2R. Based on this observation, what is the possible function of MC2RAP?**

Epidermal growth factor receptors (EGFR's) are widely expressed, and are known to control the differentiation of a variety of tissues. The EGFR family consists of four receptor isoforms (EGFR1-4) with a structure containing two extracellular cycteine-rich domain (CRD), a transmembrane segment, and an intracellular tyrosine kinase domain (TK), as depicts in Figure 1A.

EGFR1 has been implicated in gastric cancer. To gain insights into the defects associated with EGFR1, primary cultures were established from tumors and normal tissues of cancer patients, and the effect of EGF was evaluated (Figure 1B). You are assigned to investigate the possible defects associated with the mutant EGFR1, and to uncover how the aberrant receptor activity leads to gastric cancer.

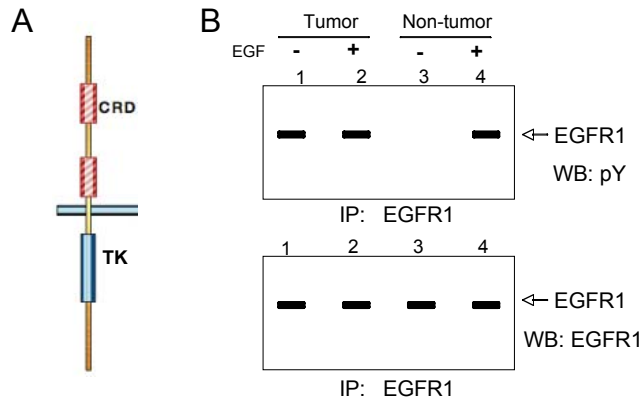


**Figure 1.** (A) Schematic diagram of a prototypical EGFR. (B) Comparison of the EGFR1 activity from tumor and non-tumor cells. Lysates (100  $\mu$ g) were used for immunoprecipitations followed by Western blotting with antibodies as indicated.

- Explain the results in Figure 1B. How does EGFR become activated under physiological conditions. Propose two possible mutations in EGFR1 that would lead to altered receptor activity as observed in Figure 1B.**
- Propose at least one experiment to uncover the molecular basis of the abnormal kinase activity of the two mutant EGFR1's, as you have hypothesized in (a).**
- The activation of EGFR1 leads to the activation of PLC-gamma, and phosphoinositol-3-kinase (PI3K). How?**
- Propose two independent experimental strategies to investigate how the activity of PLC-gamma, and phosphoinositol-3-kinase contributes to tumorigenesis of activated EGFR1.**

The gene for an orphan kinase, termed vandy kinase, was targeted in the mouse to yield a null allele. An analysis of cardiovascular function in homozygous null animals (KO) revealed no change in resting blood pressure and yielded the following results.

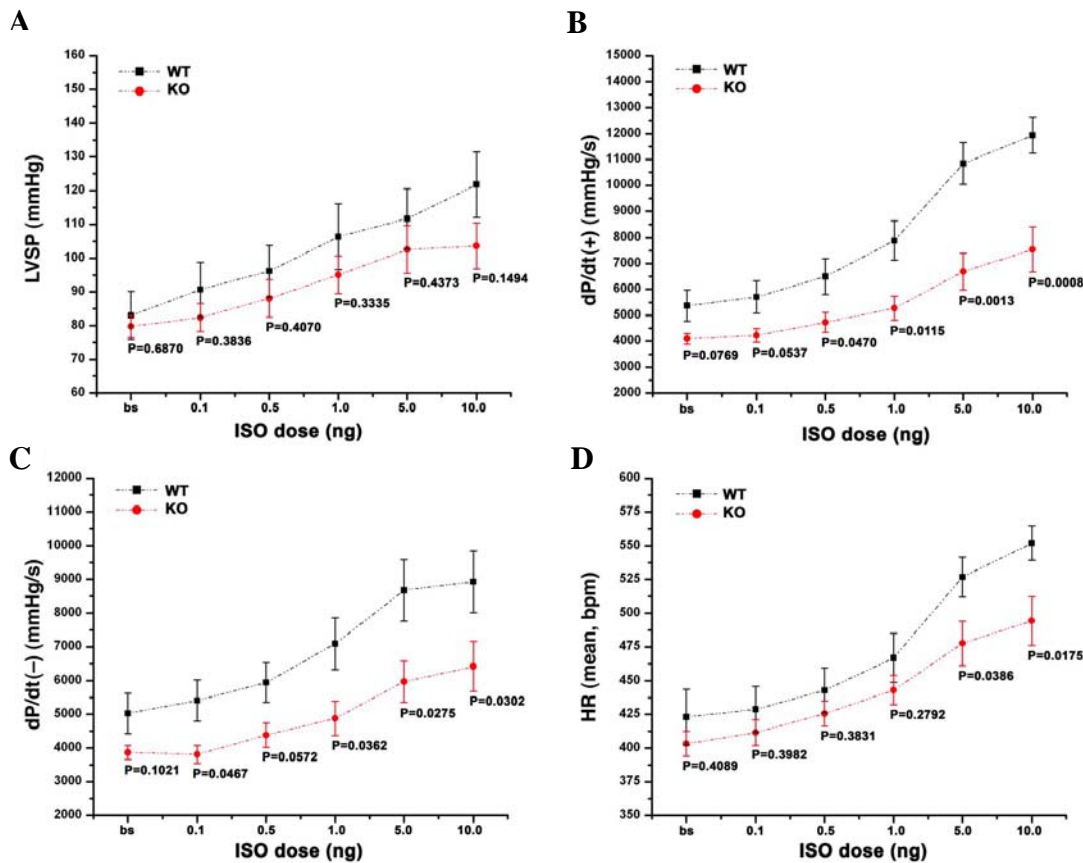


**Fig. 1. Response to graded isoproterenol (ISO) infusion in 4-month-old knockout (KO) versus wildtype (WT) mice.** Studies were in 4-month-old mice. Mice were subjected to graded isoproterenol intravenous infusion. LVSP (A), +dP/dt (B), -dP/dt (C), and heart rate (HR) (D) responses are shown. P values, comparing KO to WT mice, are displayed for each of the doses of isoproterenol. n = 8 WT and 13 KO mice. bs, basal. LVSP-Left Ventricular Systolic Pressure; dP/dt-change in pressure over time.

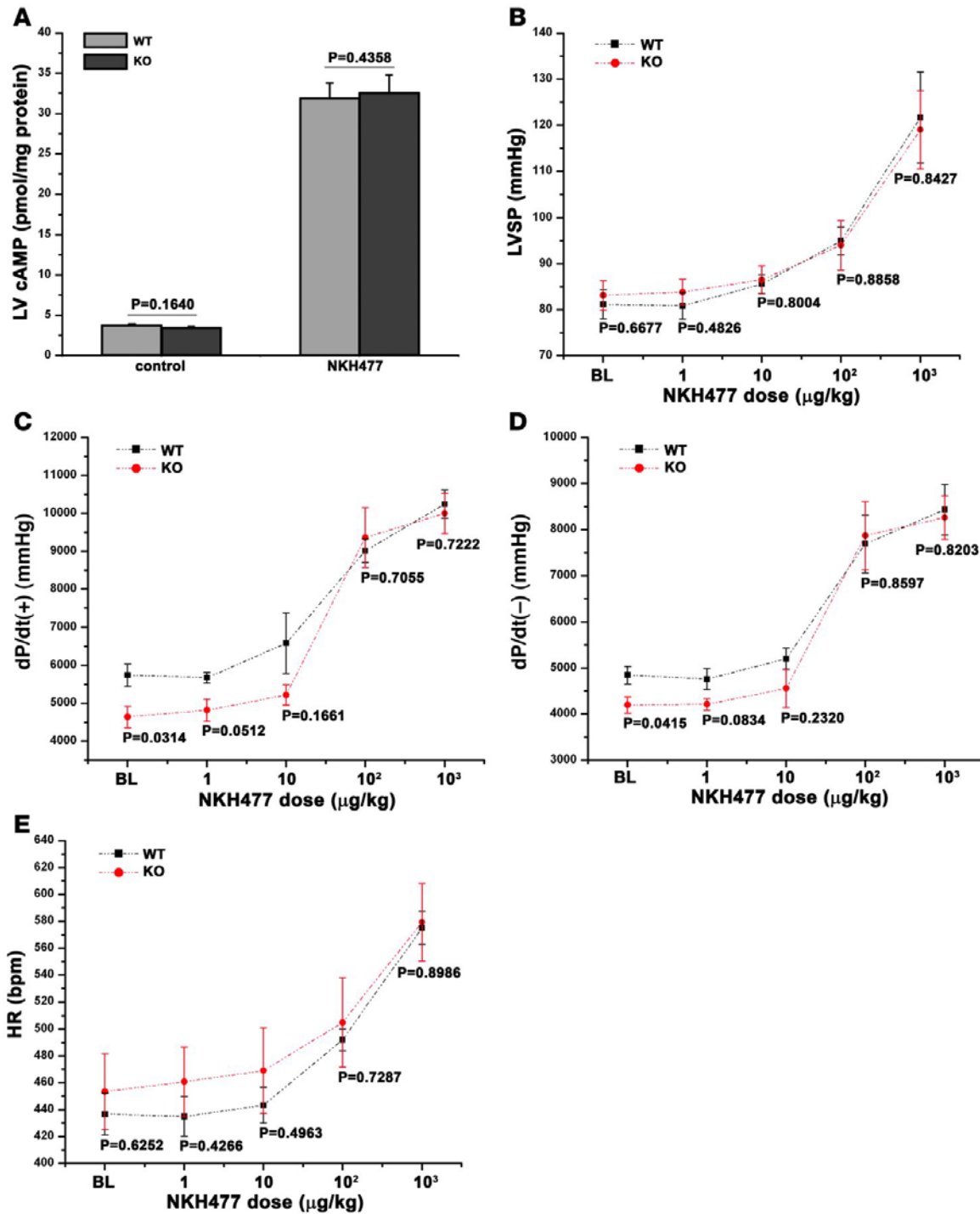


**Fig. 2. Contractile function in the KO mice following direct activation of adenylyl cyclase.** (A) cAMP production in hearts harvested from 4-month-old WT and KO animals, following graded NKH477 intravenous infusion. *n* = 5 WT and 5 KO control hearts; *n* = 7 WT and 6 KO hearts treated with NKH477. (B–E) Hemodynamic response to graded NKH477 infusion in 4-month-old animals. LVSP (B), +dP/dt (C), -dP/dt (D), and heart rate (E). BL, baseline measurement prior to administration of NKH477 versus vehicle. *n* = 9 WT and 7 KO hearts. NKH477 is a forskolin analogue.

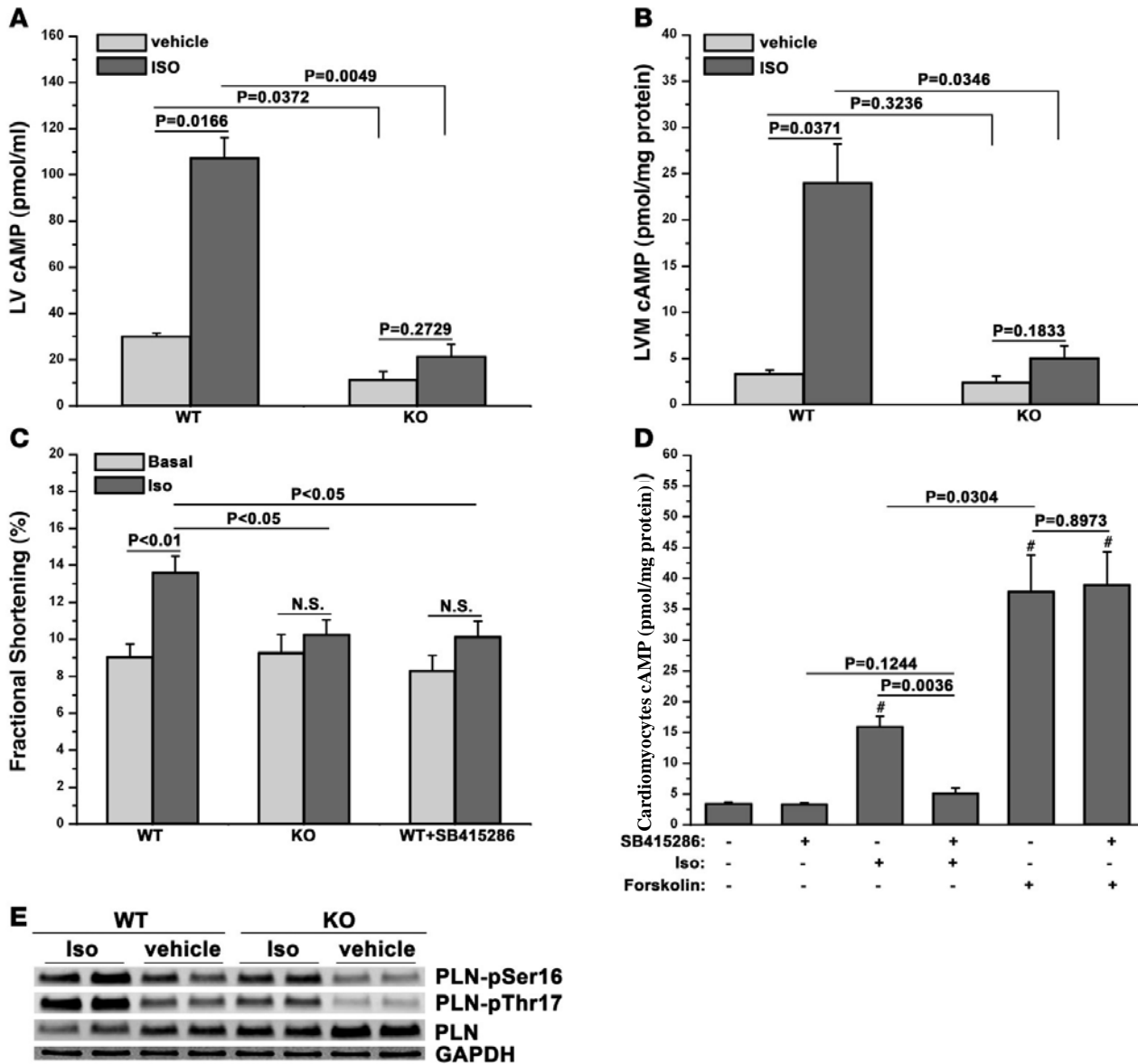


**Fig. 3. Isoproterenol-induced cAMP production.** (A–C) Studies were in 4-month-old mice. (A) cAMP production in the intact mouse heart. KO and WT mice were injected with isoproterenol (1 ng/g BW) versus vehicle. Fifteen minutes later, hearts were excised, and cAMP production was determined.  $n = 4$  mice per condition. (B) cAMP production in response to vehicle versus isoproterenol (5  $\mu$ M, 15 minutes) in cardiomyocytes isolated from KO and WT mice ( $n = 6$ ), with  $4 \times 10^5$  myocytes per assay. LVM, LV myocyte. (C) Isoproterenol-induced contractile function in the presence of a specific vandy kinase inhibitor SB415286. Cardiomyocytes were isolated from WT and KO mice ( $n = 6$ ). Fractional shortening was determined at baseline, after isoproterenol (5  $\mu$ M, 10 minutes), and in WT cells pretreated with SB415286 (10  $\mu$ M, 60 minutes).  $n = 14$  cells for WT and KO mice;  $n = 12$  cells for WT plus SB415286 mice. (D) Cardiomyocytes were pretreated with SB415286 or vehicle, followed by isoproterenol versus vehicle. (E) Isoproterenol-induced phosphorylation of phospholamban (PLN). Four-month-old WT and KO mice underwent isoproterenol infusion (1  $\mu$ g/kg BW) for 15 minutes. Lysates were immunoblotted for PLN phosphorylated at Ser16 (PKA site), Thr17 (CamKII site), total PLN, and GAPDH. BW-body weight.

**Please address the following:**

- 1) Describe the data.**
- 2) Outline your understanding of the regulation of cardiac contractility indicating where isoproterenol and forskolin analogues act, the significance of rescue by cAMP, and the role of phospholamban in regulating contractility.**
- 3) Hypothesize where the pathway regulating contractility may be dysregulated in mice lacking Vandy kinase and outline experiments to test your hypothesis.**
- 4) Vandy kinase is known to be a member of a family of kinases composed of 3 members. Inhibitors to one of the other two members of this family of kinases is now being developed for the treatment of Alzheimer's Disease. Based on the studies above, do you have any concerns on the development of such inhibitors?**

Adenosine has multiple effects on renal function. The most well studied actions involve changes in blood flow through the glomerular capillaries mediated by vasomotor effects on both afferent (pre-glomerular) and efferent (post-glomerular) arterioles. In the following experiments using isolated perfused rat kidney glomeruli, a group of investigators tested effects of adenosine A<sub>2</sub> receptor antagonists on afferent arteriole diameter (measured by videomicroscopy). The two compounds tested were SCH-58261 and MRS-1754, corresponding to A<sub>2A</sub> and A<sub>2B</sub> subtype specific antagonists, respectively. Both compounds were applied sequentially in combination with adenosine as illustrated in Fig. 1. Further, the investigators tested effects of another adenosine receptor ligand (CV-1808) that was less well characterized (Fig. 2).

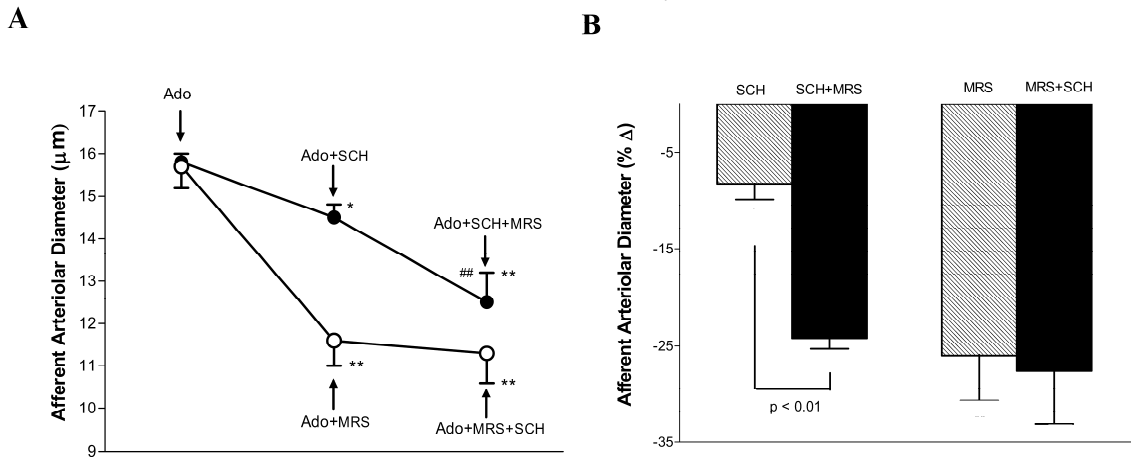


**Fig. 1** – Effects of SCH-58261 (SCH) and MRS-1754 (MRS) combined with adenosine (Ado) on afferent arteriole diameter. (A) Afferent arteriolar diameter in microns. Adenosine (10µM) was applied throughout the experiments while SCH and MRS were sequentially applied in different order. \* p<0.05 and \*\* p<0.01 vs Ado alone; # p<0.01 vs single antagonist treatment. There was no significant difference between Ado + SCH + MRS vs Ado + MRS + SCH. (B) Afferent arteriolar diameter expressed as a % change from the level observed after onset of Ado treatment.

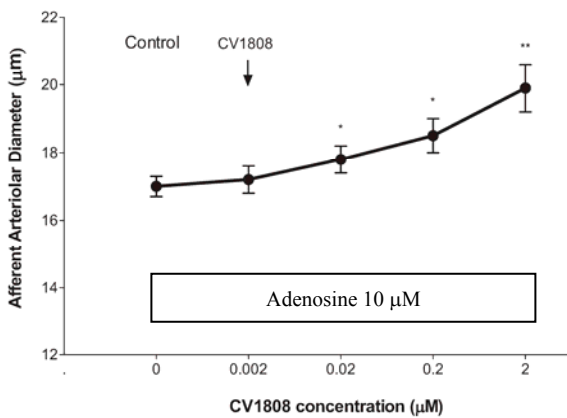


**Fig. 2** – Effects of CV-1808 on afferent arteriolar diameter. \* p<0.05 and \*\* p<0.01 vs control (no CV-1808). Adenosine (10 µM) was present throughout the experiments.

*Questions:*

- Propose at least one hypothesis to explain the data in Fig. 1.
- Develop two hypotheses to explain the action of CV-1808 on adenosine receptors. Explain how you would test these hypotheses.
- Explain how 2 µM CV-1808 would affect glomerular filtration rate under conditions of either increased or decreased extracellular fluid volume.

It is well established that  $\beta_1$  and  $\beta_2$ -adrenergic receptors ( $\beta$ ARs) on the surface of cardiomyocytes mediate distinct effects on cardiac function and the development of heart failure by regulating production of the second messenger cAMP. However, the spatial localization of  $\beta$ ARs in cardiomyocytes and the functional implications of their localization have been unclear. To address these questions, a group of investigators recently combined nanoscale live-cell scanning ion conductance microscopy (SICM) with measurements of cAMP production using a fluorescence resonance energy transfer (FRET)-based cAMP sensor. SICM is a nonoptical method in which a nanopipette is used as a scanning probe for non-contact visualization of the three-dimensional surface topography of living cells. Receptor activity is measured by monitoring the production of cAMP using the FRET-based cAMP sensor that changes its conformation and fluorescence properties upon activation (i.e. cAMP binding). In the following experiments, the FRET-based cAMP sensor was introduced into isolated cardiomyocytes from healthy rats and rats with heart failure. After acquiring an image of the cell surface topography by SICM, the investigators positioned the pipette onto various membrane regions (cell crest, T-tubule), applied the indicated receptor ligands, and recorded the FRET YFP/CFP ratio traces.

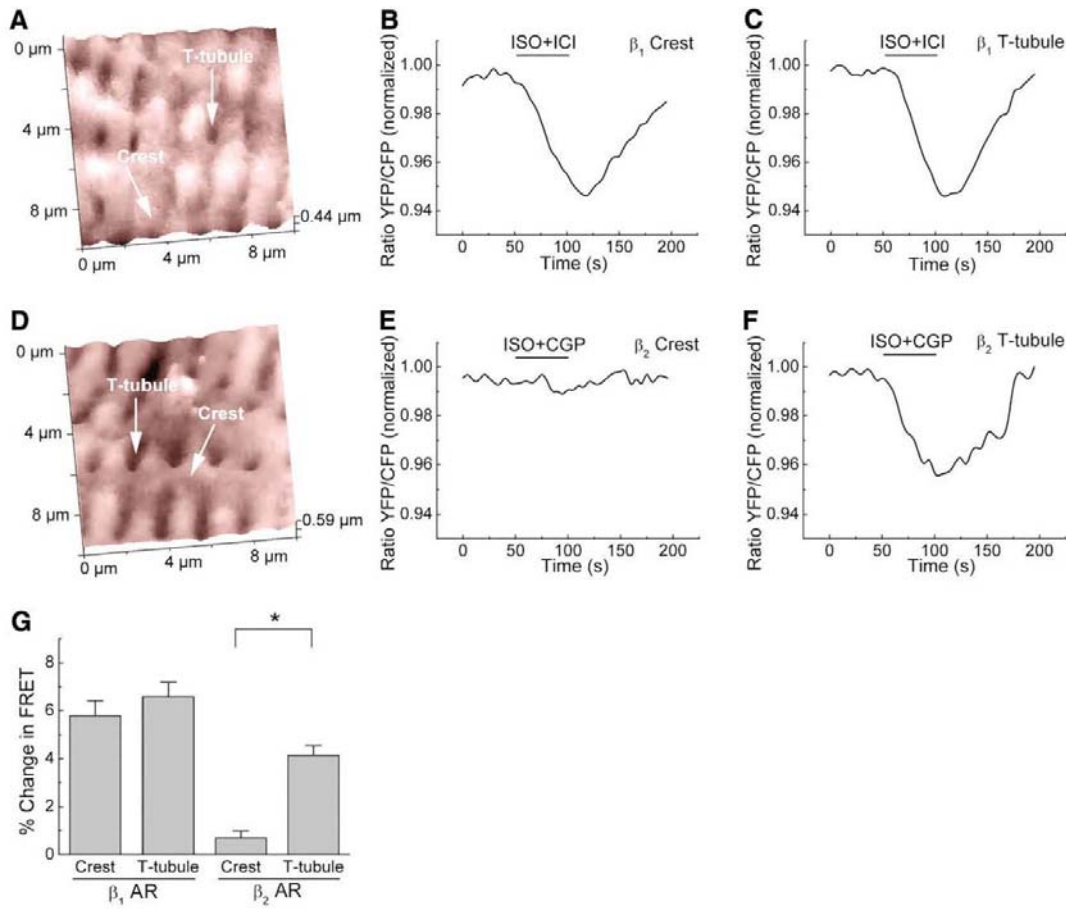


**Figure 1. Distribution of  $\beta$ AR-induced cAMP signaling in cardiomyocytes from healthy rats.** (A to C) SICM image and corresponding FRET YFP/CFP ratio traces recorded from whole cardiomyocytes after local  $\beta_1$ AR stimulation in the cell crest (B) and in the T-tubule (C), as indicated by arrows in (A). **Decrease in the FRET ratio indicates an increase in cAMP.** The cell was superfused with 50 nM of the  $\beta_2$ AR antagonist ICI118551, and  $\beta_1$ ARs were then locally stimulated from the scanning nanopipette filled with isoproterenol (ISO, 10  $\mu$ M) and ICI118551 (ICI, 5  $\mu$ M). (D to F) SICM image and corresponding ratio traces after local  $\beta_2$ AR stimulation in the cell crest (E) and in the T-tubule (F). Cells were superfused with 100 nM of the  $\beta_1$ AR antagonist CGP20712A, and then  $\beta_2$ ARs were selectively stimulated from the pipette with ISO (10  $\mu$ M) and CGP20712A (CGP, 10  $\mu$ M). (G) Quantification of the changes in FRET YFP/CFP ratios from experiments shown in (A) to (F). Data are plotted as means  $\pm$  SEM ( $n$  9). \* $P < 0.01$ , by analysis of variance (ANOVA).

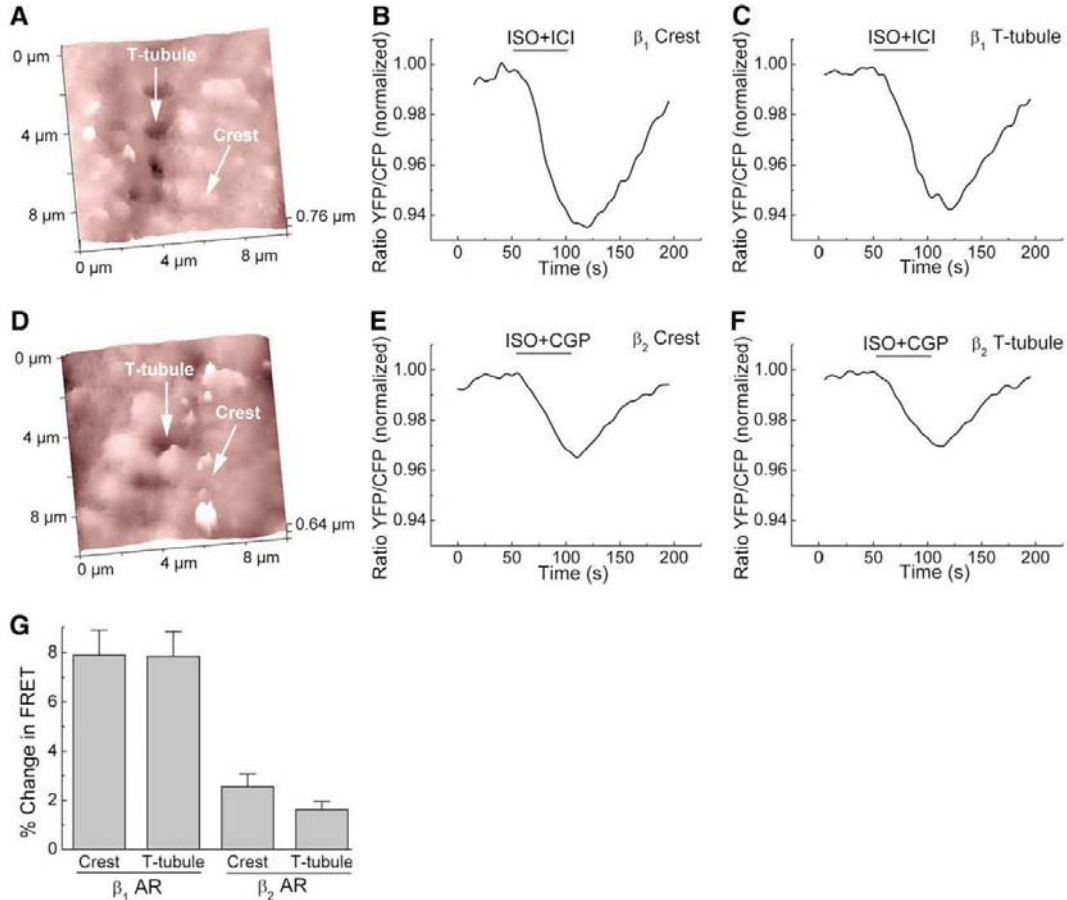
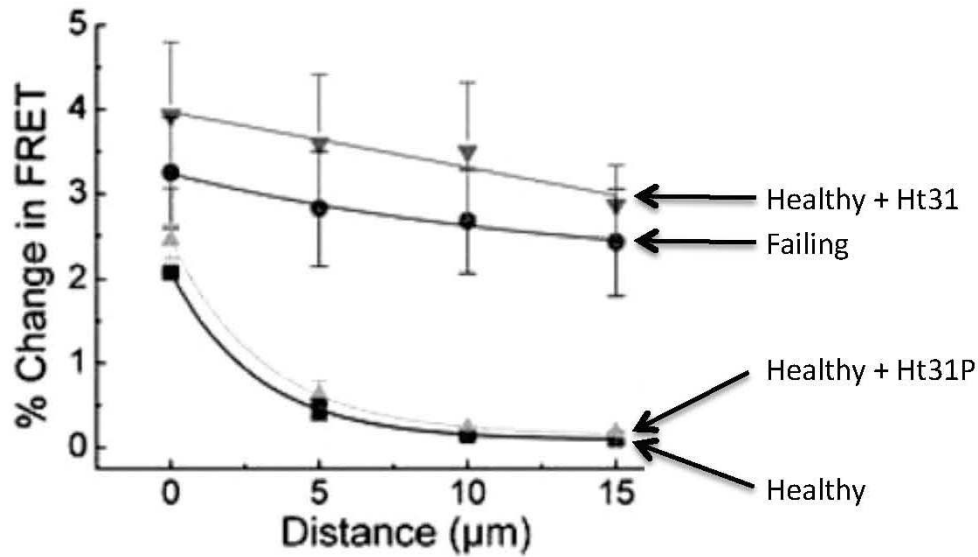


**Figure 2. Distribution of  $\beta$ AR-induced cAMP signaling in cardiomyocytes from rats with chronic heart failure. (A to C)** SICM image and corresponding FRET ratio traces after local  $\beta_1$ AR stimulation in the cell crest (B) and in the T-tubule (C). The cells were superfused and stimulated from the nanopipette as described in Fig. 1. **(D to F)** SICM image and corresponding ratio traces after local  $\beta_2$ AR stimulation in the cell crest (E) and in the T-tubule (F). **(G)** Quantification of the changes in cAMP-FRET ratios from experiments shown in (A) to (F). Data are means  $\pm$  SEM ( $n$  8).

**A. Develop a hypothesis to explain these data. Describe how the experimental results support your hypothesis.**

**B. How could your hypothesis be further tested?**

The investigators also explored the spatial organization of cAMP signaling from  $\beta$ 2ARs in normal and failing cardiomyocytes by analyzing the distribution of the FRET signals in different parts of the cell cytosol after local  $\beta$ 2AR stimulation. The experimental conditions were as follows: local stimulation of  $\beta$ 2ARs in the T-tubule of a healthy cardiomyocyte (Healthy), local stimulation of  $\beta$ 2ARs in the T-tubule of a failing cardiomyocyte (Failing), pretreatment of a healthy cardiomyocyte with 50  $\mu$ M Ht31 followed by local stimulation of  $\beta$ 2ARs in the T-tubule (Healthy + Ht31), and pretreatment of a healthy cardiomyocyte with 50  $\mu$ M Ht31P followed by local stimulation of  $\beta$ 2ARs in the T-tubule (Healthy + Ht31P). The interaction between PKA RII subunits and AKAPs is disrupted by Ht31, but not Ht31P (control). Shown below is the quantification of the cAMP signal propagation for each experimental condition. The percent change in FRET is plotted as a function of distance from the site of stimulation (0 = site of stimulation).



- C. What do these data tell you about the compartmentation of  $\beta$ 2AR-induced cAMP signaling in T-tubules?
- D. Design an experiment to test your idea.